www.elsevier.com/locate/memsci

GENERALIZED PREDICTIVE MODELING FOR FACILITATED TRANSPORT MEMBRANES ACCOUNTING FOR FIXED AND MOBILE CARRIERS

Raúl Zarca, Alfredo Ortiz, Daniel Gorri, Inmaculada Ortiz

PII: S0376-7388(17)31775-1
DOI: http://dx.doi.org/10.1016/j.memsci.2017.08.010
Reference: MEMSCI15476

To appear in: *Journal of Membrane Science*

Received date: 21 June 2017
Revised date: 27 July 2017
Accepted date: 4 August 2017

Cite this article as: Raúl Zarca, Alfredo Ortiz, Daniel Gorri and Inmaculada Ortiz, GENERALIZED PREDICTIVE MODELING FOR FACILITATED TRANSPORT MEMBRANES ACCOUNTING FOR FIXED AND MOBILE CARRIERS, *Journal of Membrane Science* http://dx.doi.org/10.1016/j.memsci.2017.08.010

GENERALIZED PREDICTIVE MODELING FOR FACILITATED TRANSPORT MEMBRANES ACCOUNTING FOR FIXED AND MOBILE CARRIERS.

Raúl Zarca, Alfredo Ortiz, Daniel Gorri, Inmaculada Ortiz*.

Department of Chemical and Biomolecular Engineering. University of Cantabria, Av. Los Castros 46, 39005 Santander, Spain

*corresponding author: ortizi@unican.es

Abstract

The present work expands previous modeling knowledge on facilitated transport membranes for olefin/paraffin separation. A new robust and practical mathematical model for the description of light olefin flux in composite polymer/ionic liquid/Ag^+ membranes is reported. The model takes into account three different transport mechanisms, i.e., solution-diffusion, fixed-site carrier and mobile carrier transport mechanisms. Fixed-site carrier contribution that appears thanks to the bounding of silver cations with the polymer chains is described through a "hopping parameter". Furthermore, given that the addition of an ionic liquid to the membrane composition promotes carrier mobility, the inclusion of a dedicated expression is necessary for a realistic description of mobile-carrier transport phenomena. The contribution of each mechanism in weighted based on the membrane composition.

In order to check the model suitability, simulated values have been matched to experimental data obtained by continuous flow propane/propylene permeation experiments through PVDF-HFP/$BMImBF_4$/$AgBF_4$ composite membranes, working with 50:50 gas mixtures at different temperature and pressure. The resultant model offers good predictions for olefin flux and provides a very useful tool for process optimization and scaling-up. To our knowledge, this is the first time that mobile and fixed site carrier mechanisms performance are simultaneously modeled considering the influence of temperature, pressure and carrier loading.

Keywords

Propylene-propane separation, facilitated transport, silver, membrane, mathematical model.

Nomenclature

A mobile carrier effective olefin diffusivity [m^2 s^{-1}]

A_m membrane effective area [m^2]

B fixed-site carrier effective olefin diffusivity [m^2 s^{-1}]

C concentration [mol L^{-1}]

D diffusion coefficient [m^2 s^{-1}]

Ea activation energy [kJ mol^{-1}]

F molar flowrate [mol s^{-1}]

H Henry's solubility constant [mol bar^{-1} m^{-3}]

ΔH_{sol} Henry's constant enthalpy [kJ mol^{-1}]

J molar flux [mol m^{-2} s^{-1}]

K_{eq} equilibrium constant [m^3 mol^{-1}]

K_H fixed carrier effective permeability [mol bar^{-1} m^{-1} s^{-1}]

K_p heterogeneous equilibrium constant [bar^{-1}]

L membrane thickness [m]

P permeability [mol bar^{-1} m^{-1} s^{-1}]

p pressure [bar]

R universal gas constant [8.314 J mol^{-1} K^{-1}]

ΔH_r complexation reaction enthalpy [kJ mol^{-1}]

S gas solubility [mol bar^{-1} m^{-3}]

T temperature [K]

X mole fraction [-]

x membrane thickness dimension [m]

Greek letter

α fitting parameter

Superscript / subscript

0 feed side

C_3H_6 propylene

C_3H_8 propane

comp organometallic complex

D organometallic complex diffusion

eq chemical equilibrium

FC fixed-site carrier

IL ionic liquid

L permeate side

N_2 nitrogen

m membrane

MC mobile carrier

r reaction

ref reference

SD solution-diffusion

1. Introduction

The separation of light olefin/paraffin mixtures has been recently defined as one of the key chemical separations that can bring great global benefits once improved. Replacing traditional distillation by new processes that do not require a phase change could lower the energy intensity of the process by a factor of ten [1]. In this sense, membrane technology offers a modular and cost-effective solution able to reduce the energy demand of the separation process by means of process intensification [2].

Several approaches have been reported to synthesize effective olefin/paraffin separation membranes. The simplest way is to exploit the intrinsic separation properties of polymers in a dense membrane configuration. Dense polymeric membranes made of glassy, rubbery and cellulosic polymers perform high selectivities at the expense of low permeabilities [3–6]. More recently, new materials have been tested for their application in alkane/alkene separation, including polymers with intrinsic microscopy [7,8], metal-organic frameworks [9,10], carbon molecular sieves [11,12] and graphene [13], displaying a wide distribution of results.

However, the intrinsic separation properties of polymers are vastly improved when a metallic cation with the ability to reversibly and selectively react with the olefin is dissolved in the polymer matrix, resulting in the facilitated transport mechanism [14]. In this context, silver cations are known for their capability to form stable complexes with the olefin via π-bonding mechanism [15,16].

Gas separation based on facilitated transport has been approached working in liquid phase, mainly in the form of supported liquid membranes [17–20], but their poor mechanical stability and the solvent losses by evaporation are major drawbacks for real industrial application, especially when subjected to pressure gradients [21]. In order to overcome this handicap, the use of ionic liquids as liquid phase has been recently

assessed [22]. Besides their negligible vapor pressure, ionic liquids are non-flammable excellent solvents whose chemical and physical properties can be tailored by a judicious selection of cation, anion, and substituents [23,24].

The unique properties of ionic liquids can be used to improve membrane performance in polymer electrolyte membranes. On the one hand, the presence of an ionic liquid within the free volume of the polymer promotes mobility among the silver cations which, after binding to the olefin, will diffuse through a mobile-carrier transport mechanism [25]; in this way, the characteristic fixed-carrier "percolation threshold" is avoided and facilitated transport occurs even at low silver concentrations [26]. On the other hand, the lack of volatility of ionic liquids mitigates the stability issues produced by solvent evaporation during the first operating hours. In addition, it is remarkable that silver ions are more stable when surrounded by ionic liquid molecules [16,27,28].

Composite facilitated transport membranes prepared by introducing a room temperature ionic liquid inside the polymer electrolyte free volume, have shown great performance for olefin/paraffin separation, easily surpassing the trade-off between permeability and selectivity for polymeric membranes [29]. Several approaches have been assessed, including the use of polymerized ionic liquids as polymeric matrix [30]. The internal structure of a composite membrane consists of a polymeric matrix with the ionic liquid molecules entrapped within the free volume. The silver cations are distributed; some are bonded to the polymer electronegative atoms while others are solvated by the ionic liquid. In the first case, the olefin "hops" from a cation site to a different cation site in a sequence of complexation-decomplexation steps, achieving a net flux thanks to the activity gradient [31,32]. In the second case, the whole Ag^{+}-olefin complex diffuses through the ionic liquid domains existing within the polymer free volume [22].

The use of membranes to carry out this separation has been modeled for various materials and configurations. Regarding polymeric membranes, Najari et al. [33] studied and compared several models, including the frame of reference/bulk flow and Maxwell-Stefan models for polyimide membranes, while Sridhar and Khan [34] and Castoldi et al. [35] developed mathematical models focusing on industrial membrane configurations.

Regarding facilitated transport membranes, their promising performance has promoted several works on mathematical modeling to explain the transport phenomena in solid-state membranes; being the most recognized the dual sorption model [36,37], the limited mobility of chained carriers model [38,39] and the concentration fluctuation model [40,41]. In addition, mobile carrier facilitated transport in the liquid phase has been previously modeled for several separation systems as nitric oxide in ferrous chloride solutions [42] and enriched-air production [43]. However, all of them find their application in membranes that ~~only~~ perform according to one facilitated transport mechanism, making them unsuitable for composite membranes that perform according to hybrid mobile/fixed carrier transport.

In this work, the main goal is to develop a general and broadly applicable mathematical model able to describe the olefin flux through polymer-IL composite membranes as a function of the membrane composition and operating conditions. The model expresses the total flux as a sum of the contributions caused by the three mentioned mechanisms. A new expression to define the fixed-site carrier effective permeability through a “hopping parameter” is used along with the mathematical expressions for mobile carrier and solution-diffusion mechanisms. The model contains two fitting parameters that have been estimated using modeling software, fitting the mathematical model to experimental data.

The experimental values have been obtained by continuous flow propane/propylene gas-mixture permeation experiments on composite membranes made of PVDF-HFP, the ionic liquid 1-butyl-3-methylimidazolium tetrafluoroborate ($BMImBF_4$) and $AgBF_4$ silver salt. The separation capability of this membrane composition had been previously checked by this research group [29] but the polymer/ionic liquid ratio has been optimized for the experimental section of this work. The imidazolium-based $BMImBF_4$ ionic liquid was selected based on previous screening works that revealed a proper propylene solubility and good miscibility with the PVDF-HFP fluoropolymer [44]. The use of a silver salt with the same anion as the ionic liquid intends to reduce the number of chemical species in the composite membranes, hence reducing its complexity. Finally, the PVDF-HFP fluoropolymer presents moderate crystallinity [45], which is related to the low physical solubility of the gaseous species. Therefore, as the olefin sorption is vastly enhanced by the chemical complexation, the use of a low permeable polymer in conjunction with facilitated transport results in very high selectivities and permeabilities. In addition, PVDF-HFP presents remarkable mechanical, thermal and chemical stability.

As opposed to previous models reported in the literature, this model is able to simulate the three transport mechanisms simultaneously acting in the membrane, weighting at the same time their relative contribution. Therefore, the reported model provides a useful predictive tool to be applied in such systems where fixed-site carrier and mobile carrier transport mechanisms coexist, thus simplifying the optimization and scaling-up of composite membranes-based separation units.

2. Experimental

2.1 Chemicals

Propylene and propane gases were purchased from Praxair with a purity of 99.5% for both gases. Poly(vinylidene fluoride-co-hexafluoropropylene) (PVDF-HFP) was supplied by Sigma Aldrich. The ionic liquid $BMImBF_4$ with a minimum purity of 99% and a halide content of less than 500 ppm was provided by Iolitec. Silver tetrafluoroborate ($AgBF_4$) with a minimum purity of 99% was purchased from Apollo Scientific Ltd. Tetrahydrofuran (THF) was supplied by Panreac and was used as solvent for membrane synthesis. All chemicals were used as received with no further purification.

2.2 Membrane synthesis

The composite membranes for the experimental tests were prepared by the solvent casting method. The desired amount of PVDF-HFP was dissolved in THF using a 10 mL sealed glass vial to avoid solvent losses by evaporation. The content was stirred during 24 h at room temperature. To achieve complete dissolution of the polymer, the mixture was subjected to a heating step at 50 ºC during 5 minutes. After that, the selected amounts of ionic liquid and silver salt were added to the solution and the whole mixture was stirred at room temperature during 15 minutes. The membrane precursor was poured in a glass dish and then introduced in a vacuum oven overnight at 800 mbar and 25 ºC. Finally, a more severe evaporation step at full vacuum (~1 mbar) during 1 hour was performed for further solvent removal. Light exposure was avoided during the whole synthesis process to prevent silver reduction. The resulting thickness of the prepared dense films was around 100 μm. For calculation purposes, the real thickness of

each membrane was measured using a digital micrometer Mitutoyo Digimatic MDC-25SX (accuracy ± 0.001 mm).

2.3 Gas permeation experiments

The gas permeation experiments were conducted using the gas-mixture continuous-flow technique. A complete description of the permeation method has been included in previous works [29]. Essentially, the membrane was placed in a steel permeation cell and the desired olefin/paraffin mixture was passed through the upper chamber. Nitrogen was used as sweeping gas through the permeate side. The cell was located in a temperature-controlled oven. The feed and permeate streams were analyzed using a gas HP 6890 chromatograph equipped with a thermal conductivity detector (TCD). A simple mass balance allows calculating the experimental flow of each gaseous species through the membrane:

$$J_{C_3H_X} = \frac{1}{A_m} \frac{x_{C_3H_X}}{x_{N_2}} F_{N_2} \quad (1)$$

Where A_m is the effective membrane area, $x_{C_3H_X}$ and x_{N_2} are the gaseous species mole fractions, respectively, in the permeate chamber outlet stream and F_{N_2} is the nitrogen molar flow rate. The permeation experiments were conducted at the experimental conditions shown in Table 1, where the studied variables are the temperature, ranging from 293 to 303 K, the feed pressure, ranging from 1 to 3 bar and the membrane silver loading from 1.3 to 5.2 mol·L^{-1}.

Table 1. Experimental conditions

Experimental condition	Value
T (K)	293-303
Permeation area (cm^2)	53
N_2 flow (mL min^{-1})	20
C_3H_6 flow (mL min^{-1})	15
C_3H_8 flow (mL min^{-1})	15
C_3H_8 /C_3H_6 feed gas ratio	50:50
Feed side pressure (bar)	1-3
Permeate side pressure (bar)	1
Silver concentration (mol·L^{-1})	1.3-5.2
Polymer/ionic liquid mass ratio	80:20

2.4 Membrane morphology characterization

Scanning electron microscopy (Carl Zeiss EVO MA 15) was employed to observe the cross-section and surface morphology of the synthesized membranes. The samples were prepared by liquid nitrogen fracturing to avoid altering the sectional morphology, followed by gold sputtering in a Balzers Union SCD040 sputter coating system. The line-scan spectrum of energy dispersive X-ray spectroscopy (EDX) was applied to the same samples of SEM to assess the silver dispersion profile in the membrane cross-section.

3. Mathematical Modeling

The gas transport mechanisms occurring inside the membrane are the result of the complex membrane structure. In the reported model, we approach the complexity of the composite membrane structure by simplifying its nature, considering that the transport mechanism is shared between fixed site and mobile carrier, accounting for bounded and unbounded silver cations, respectively. On the one hand, fixed-site carrier mechanism appears when the silver cations bind to polymer atoms that can donate electrons and stabilize (i.e. fluorine atoms present in PVDF-HFP backbone). Experimental studies in the literature report the capability of fluorine atoms in C-F groups to form coordination bonds with cations as Ag^+ [46,47]. In this regard, PVDF-HFP has been previously reported for the preparation of polymer electrolytes by blending with HBF_4, resulting in the proton coordination with the polymer fluorine atoms [48]. The $AgBF_4$ solubility in a polymer matrix by means of coordination with the electron-donor atoms of the polymer chains has been also reported [49]. On the other hand, the presence of ionic liquid molecules within the free volume of the polymer facilitates the existence of unbound silver cations with higher freedom to diffuse. When the olefin complexes with one of these silver cations, the whole organometallic complex diffuses through the membrane. This transport mechanism is known as “mobile carrier”. A schematic representation of the transport mechanisms is depicted in Figure 1.

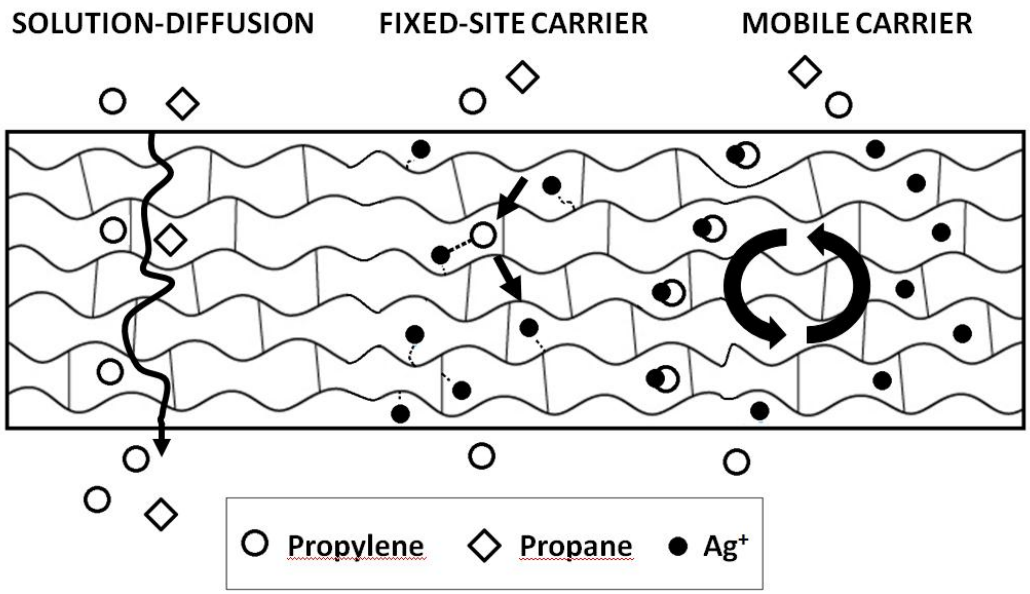

Figure 1. Schematic representation of the gas transport mechanisms.

The total propylene flux through the membrane may be calculated as the sum of the contribution of each transport mechanism [32]:

$$J_{C_3H_6} = -D_{C_3H_6,m}\frac{dC_{C_3H_6}}{dx} - A\frac{dC_{C_3H_6}}{dx} - B\frac{dC_{C_3H_6}}{dx} \quad (2)$$

The parameters A and B represent the "effective diffusivity" of the organometallic complex specie in the mobile carrier and fixed-site carrier mechanisms respectively. Equation 2 can be integrated along the membrane domain:

$$J_{C_3H_6} = D_{C_3H_6,m}\frac{C^0_{C_3H_6} - C^L_{C_3H_6}}{L} + A\frac{C^0_{C_3H_6} - C^L_{C_3H_6}}{L} + B\frac{C^0_{C_3H_6} - C^L_{C_3H_6}}{L} \quad (3)$$

Where subscripts 0 and L refer to feed and permeate sides, respectively. If sorption equilibrium at the interphase is assumed, Equation 3 can be reformulated as:

$$J_{C_3H_6} = D_{C_3H_6,m}\cdot S_{C_3H_6,m}\frac{p^0_{C_3H_6} - p^L_{C_3H_6}}{L} + P_{comp}\frac{p^0_{C_3H_6} - p^L_{C_3H_6}}{L} + K_H\frac{p^0_{C_3H_6} - p^L_{C_3H_6}}{L} \quad (4)$$

Where P_{comp} is the permeability of the olefin based on the olefin-silver complex transport and K_H acts as an effective permeability or "hopping parameter" for the olefin *via* fixed site carrier mechanism. The diffusivity and solubility values of propylene in the PVDF-HFP/$BMImBF_4$ matrix have been reported previously [50]; however, in many cases, the contribution of the solution-diffusion mechanism can be neglected compared with that caused by facilitated transport.

The permeability of the olefin-silver complex attributed to the mobile carrier mechanism is the product of its diffusivity in the ionic liquid times its chemical solubility; this latter parameter can be obtained from the complexation reaction between the silver cations and the propylene as follows [27]:

$$Ag^+ + C_3H_6 \overset{Keq}{\leftrightarrow} Ag^+(C_3H_6) \quad (5)$$

The equilibrium constant can be expressed as:

$$k_{eq} = \frac{\left[Ag^+(C_3H_6)\right]}{\left[Ag^+\right]\cdot\left[C_3H_6\right]} \quad (6)$$

While the concentration of free cations is given by:

$$\left[Ag^+\right] = \left[Ag^T\right] - \left[Ag^+(C_3H_6)\right] \quad (7)$$

Solving for the complex specie concentration:

$$\left[Ag^+(C_3H_6)\right] = \frac{k_{eq}\left[Ag^T\right]\cdot\left[C_3H_6\right]}{1 + k_{eq}\left[C_3H_6\right]} \quad (8)$$

Furthermore, after the relationship between the concentration of propylene physically absorbed and the partial pressure in the gas phase through a Henry type isotherm the resulting equation is:

$$\left[Ag^{+}\left(C_3H_6\right)\right]=\frac{k_{eq}\left[Ag^{T}\right]\cdot p_{C_3H_6}H_{C_3H_6}}{1+k_{eq}p_{C_3H_6}H_{C_3H_6}} \quad (9)$$

So that the ratio between the organometallic complex concentration and the propylene partial pressure in the gas phase, i.e. a chemical solubility coefficient, can be obtained as:

$$S_{C_3H_6,chem}=\frac{k_{eq}\left[Ag^{T}\right]\cdot H_{C_3H_6}}{1+k_{eq}p_{C_3H_6}H_{C_3H_6}} \quad (10)$$

Finally, the olefin permeability through the mobile carrier mechanism can be expressed as:

$$P_{comp}=\frac{k_{eq}\left[Ag^{T}\right]\cdot H_{C_3H_6}}{1+k_{eq}p_{C_3H_6}H_{C_3H_6}}\cdot D_{comp} \quad (11)$$

Where the equilibrium constant k_{eq}, the physical solubility of the propylene in the ionic liquid $H_{C_3H_6}$, the olefin-paraffin complex diffusivity D_{comp}, and the influence of temperature on these parameters have been reported in previous works [22,27]:

$$H_{C_3H_6}=H_{C_3H_6,0}e^{\frac{-\Delta H_{sol}}{RT}} \quad (12)$$

$$\ln\frac{k_{eq}}{k_{eq,ref}}=-\frac{\Delta H_r}{R}\left(\frac{1}{T}-\frac{1}{T_{ref}}\right) \quad (13)$$

$$D_{comp}=D_{comp,ref}e^{-\frac{Ea_D}{R}\left(\frac{1}{T}-\frac{1}{T_{ref}}\right)} \quad (14)$$

In addition, it should be taken into account that the transport flux due to the fixed site carrier mechanism, characterized by the "hopping parameter" K_{FC}, is a function of the silver loading in the membrane and the temperature [51]. A mathematical expression can be derived for the dependence of K_{FC} on temperature and silver concentration. The concentration of free cations ready to coordinate with propylene molecules to form the coordination complex can be derived from the chemical equilibrium. In this regard, the heterogeneous complexation reaction between propylene and silver cations bound to the polymer matrix is depicted by the following equation:

$$\left[Ag^{+}\right] + P_{C_3H_6} \overset{k_p}{\leftrightarrow} \left[Ag^{+}\left(C_3H_6\right)\right] \quad (15)$$

Again, the equilibrium constant can be expressed as:

$$k_p = \frac{\left[Ag^{+}\left(C_3H_6\right)\right]}{\left[Ag^{+}\right] \cdot p^{0}_{C_3H_6}} \quad (16)$$

Introducing Equation 7 and solving for the free silver cations concentration:

$$\left[Ag^{+}\right] = \frac{\left[Ag^{T}\right]}{1 + k_p p^{0}_{C_3H_6}} \quad (17)$$

The proportionality between the value of K_{FC} and the variables is defined through the fitting parameter α:

$$K_{FC} = \alpha \left(\frac{\left[Ag^{T}\right]}{1 + k_P \cdot p^{0}_{C_3H_6}} \right) e^{\frac{Ea_{FC}}{R}\left(\frac{1}{293} - \frac{1}{T}\right)} \quad (18)$$

In Equation 18 the influence of temperature in the hopping mechanism has been described through an Arrhenius-type expression, and the term in brackets refers to the concentration of free "uncomplexed" silver cations, as obtained from the heterogeneous

chemical equilibrium, Equation 16. The value of the heterogeneous equilibrium constant has been taken from previous works based on the fixed-site carrier mechanism [51]. The parameter α and the activation energy of the hopping parameter (Ea_{FC}) are the two fitting parameters of the model.

To summarize, the propylene flux is described as the sum of three contributions as follows:

$$J_{C_3H_6} = J_{C_3H_6,SD} + J_{C_3H_6,MC} + J_{C_3H_6,FC} \quad (19a)$$

$$J_{C_3H_6,SD} = D_{C_3H_6,m} \cdot S_{C_3H_6,m} \frac{p^0_{C_3H_6} - p^L_{C_3H_6}}{L} \quad (19b)$$

$$J_{C_3H_6,MC} = \frac{k_{eq}[Ag]H_{C_3H_6}}{1 + k_{eq} p_{C_3H_6} H_{C_3H_6}} \cdot D_{comp} \frac{p^0_{C_3H_6} - p^L_{C_3H_6}}{L} x_{IL} \quad (19c)$$

$$J_{C_3H_6,FC} = K_{FC} \frac{p^0_{C_3H_6} - p^L_{C_3H_6}}{L} (1 - x_{IL}) \quad (19d)$$

The contribution of the two different mechanisms of facilitated transport mechanism has been weighted based on the mass fraction of ionic liquid in the membrane composition x_{IL}. This approach assumes that the available silver cations are distributed according to the polymer/ionic liquid mass ratio and homogeneously dispersed as observed in EDX analysis.

The propane flux is caused by simple Fickian diffusion along the membrane, as described by the following equation:

$$J_{C_3H_8} = D_{C_3H_8,m} \cdot S_{C_3H_8,m} \frac{p^0_{C_3H_8} - p^L_{C_3H_8}}{L} \quad (20)$$

With the exception of the fitting parameters, α and Ea_{FC}, the values of model parameters have been extracted from previous works. In the case of mobile carrier, the values of the organometallic complex diffusivity and its dependence on temperature were taken from an experimental study on supported ionic liquid membranes (SILMs). These membranes where synthesized introducing the $BMImBF_4/AgBF_4$ mixture in the pores of a hydrophilic PVDF support [22]. The value of the equilibrium constant for the complexation reaction, the propylene solubility in the ionic liquid, and their enthalpies were extracted from absorption equilibria of propylene in ionic liquid/Ag^+ solutions [27]. The value of the heterogeneous equilibrium constant was calculated in a previous study on fixed site carrier mechanism [51].

It is worth noticing that the values of the estimated parameters are dependent on the chemical nature of the involved species (permeant gas, polymer, carrier and ionic liquid) and the interactions between them. As a result, the procedure to implement this model in similar hybrid systems implies the use of case-specific model parameters and the estimation of a new pair of values for both α and Ea_{FC}.

4. Results and discussion

4.1 Membrane morphology

Figure 2 shows the cross-section and surface of a PVDF-HFP membrane, a PVDF-HFP/$BMImBF_4$ membrane and a composite PVDF-HFP/$BMImBF_4$/$AgBF_4$. The cross-section micrographs show a non-porous homogenous structure without cavities or voids in all three cases. There is no evidence of pure ionic liquid domains in membranes **B** and **C**, proving the complete mixture between the ionic liquid and the polymer. Furthermore, the addition of the silver salt in membrane **C** does not modify the structure but maintains the original dense and homogeneous pattern.

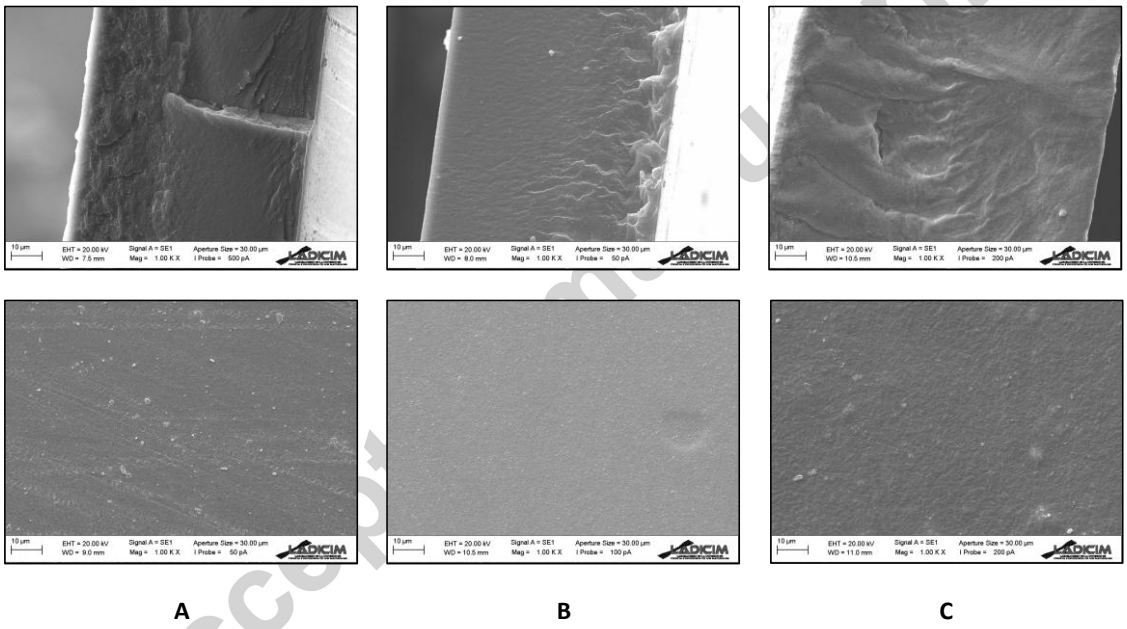

Figure 2. Cross-section and surface morphology of: A) PVDF-HFP membrane B) PVDF-HFP/$BMImBF_4$ membrane, C) PVDF-HFP/$BMImBF_4$/$AgBF_4$ 5.2 mol/L.

Further knowledge on membrane structure can be extracted from the EDX analysis. EDX makes use of x-ray spectrum emitted by the solid sample bombarded with a focused beam of electrons to obtain a localized chemical analysis. When the sample is

hit by the electron beam, electrons are ejected from the atoms of the sample's surface. The resulting electron vacancies are filled by electrons from a higher energy state, and an x-ray is emitted to balance the energy difference between the two electrons' states. The x-ray energy is characteristic of the element from which it was emitted.

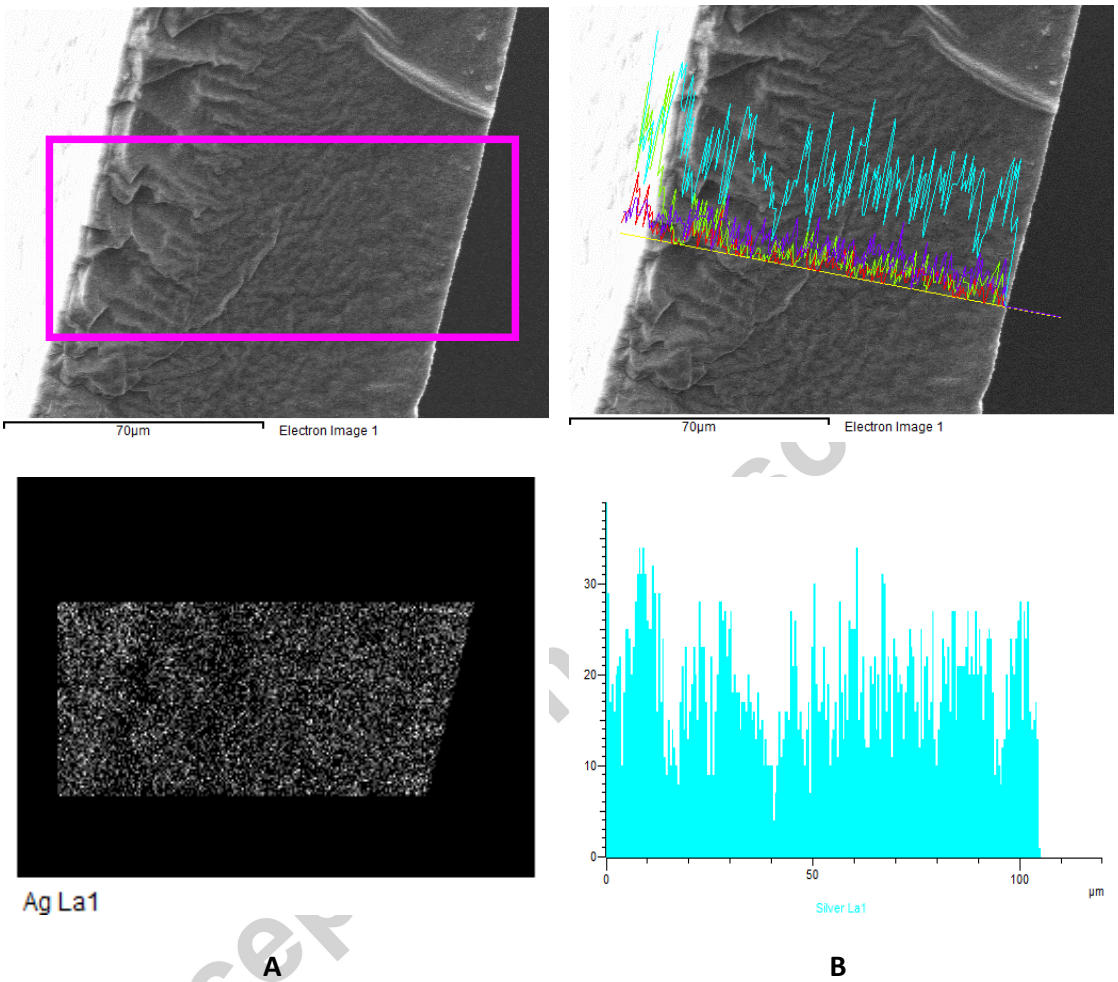

Figure 3. Energy dispersive X-Ray spectroscopy patterns of silver in the PVDF-HFP/BMImBF$_4$/AgBF$_4$ 5.2 mol/L membrane: A) dispersion plot, B) scan-line.

In this work, EDX was used in conjunction with SEM to obtain scan-lines and plot-mapping patterns of elemental silver on cross-sectional images of the composite membrane. The energy dispersive x-ray spectroscopy patterns shown in Figure 3

confirm that no ionic aggregates or silver particles are formed inside the membrane, which is in good agreement with the previous discussion on silver salt dissolution. Thus, the silver is homogeneously dispersed along the membrane thickness with no layers of preferential accumulation.

4.2 Permeation results

Table 2 displays the experimental performance of the composite membranes assessed in this work. The experimental effective permeability has been calculated normalizing the experimental flux with the membrane thickness and the partial pressure gradient, as shown in Equation 21.

$$P_{C_3H_X} = J_{C_3H_X} \frac{L}{\Delta p_{C_3H_X}} \quad (21)$$

Facilitated transport phenomena yielded remarkably high values of propylene permeability. On the other hand, the composite material causes very low propane permeability, as it is only due to Fickian diffusion. As a result, the membrane provides remarkably high separation selectivity values. The results show that the propane permeability suffers a slight increase as the silver loading rises. Although the behavior of the paraffin is unusual, similar behavior has been observed in some previous studies, such as those reported by Kim et al. [52] and Surya Murali et al. [53].

Table 2. Experimental permeability and propylene/propane selectivity at 293K and 0.5 bar feed partial pressure of each gas.

[Ag] (M)	P C_3H_8 (Barrer)	P C_3H_6 (Barrer)	$\alpha_{i/j}$
1.31	6.1	890	146
2.62	10.8	1374	127
3.92	14.4	2342	163
5.23	24.7	3291	133

Figure 4 depicts the influence of the feed partial pressure on the experimental olefin flux. As the partial pressure gradient offers the driving force of the separation process, it has a direct effect on the propylene flux. Nonetheless, the composite membrane performs high olefin fluxes even at the lower assessed partial pressures, forecasting its suitability for the separation of other olefin/paraffin mixtures with minor presence of the olefin. On the other hand, the effect of the temperature increase on the propylene flux is also depicted in Figure 4. The resulting higher flux at 303 K is mainly caused by the positive effect of temperature on the organometallic complex diffusivity. Although the solubility of the gaseous species decreases at higher temperatures and the complexation equilibrium constant is negatively affected by the temperature, these effects are hindered by the diffusivity influence on the permeation process [50].

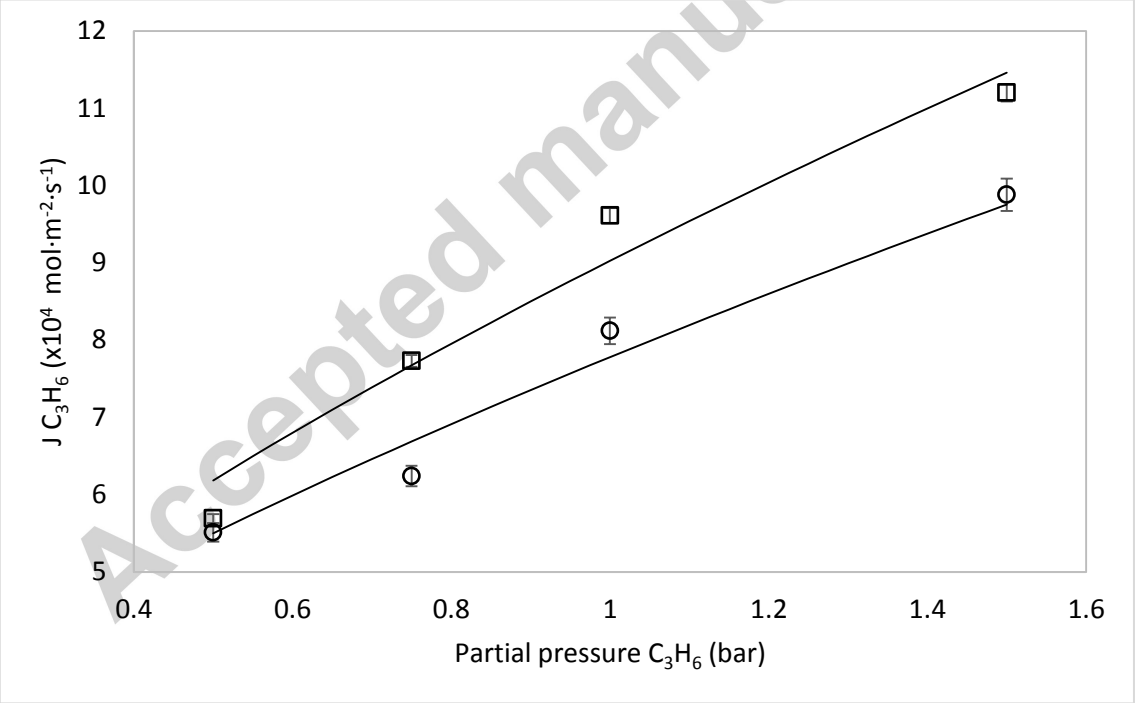

Figure 4. Experimental and predicted propylene flux in the PVDF-HFP/BMImBF$_4$/AgBF$_4$ 5.2 mol/L membrane at 293 (○) and 303K (□) with increasing partial pressure.

The non-linear trend observed in Figure 4 is an indication that a selective reaction is taking place within the membrane, which is consistent with the facilitated transport mechanism. It is a well known behavior in facilitated transport membranes that the partial pressure markedly influences the permeability of the gas that interacts with the carrier [47]. Taking into account that the permeability has been defined as a phenomenological parameter by means of Equation 21, the values calculated from the experimental fluxes are shown in Figure 5. A typical behavior of facilitated transport membranes can be seen, characterized by a decreasing permeability value with the olefin partial pressure as the carrier becomes saturated.

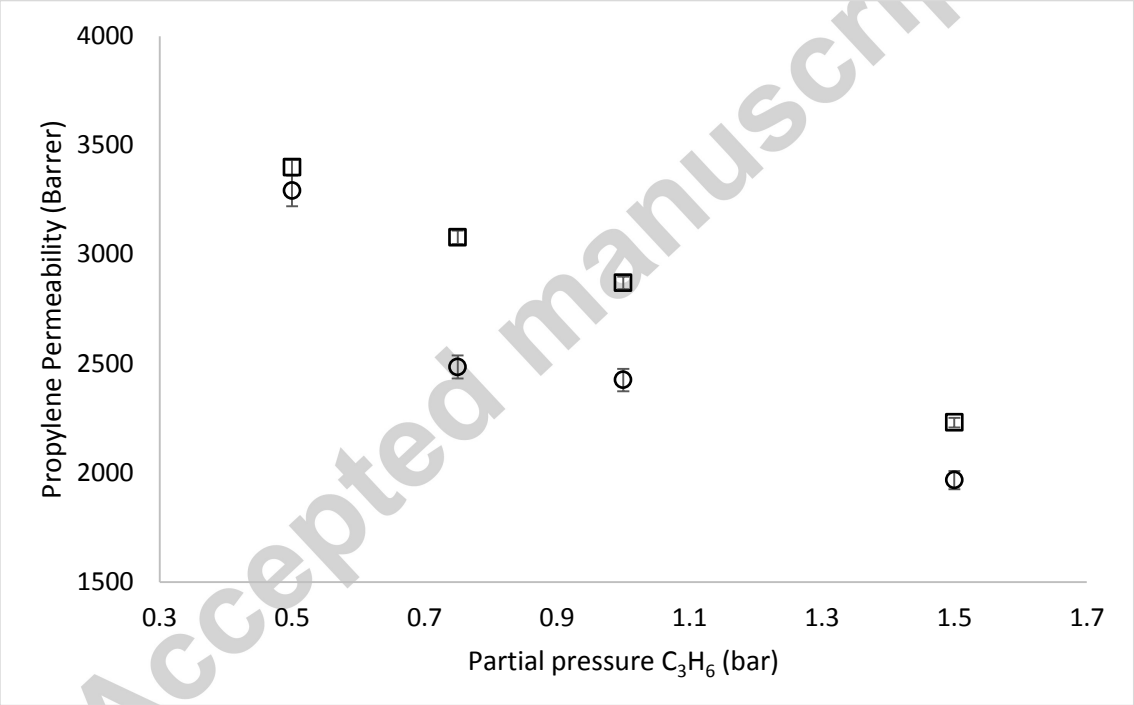

Figure 5. Propylene permeability at 293 (○) and 303 K (□) with increasing feed partial pressure in the PVDF-HFP/BMImBF$_4$/AgBF$_4$ 5.2 mol/L membrane.

The effect of silver concentration on the propylene flux is shown in Figure 6. A linear increase of the experimental flux is clearly observed with increasing silver concentration. As opposed to polymer electrolyte membranes, ionic-liquid-containing

composite membranes do not perform the characteristic "percolation threshold" [26,51,54,55]. This effect is caused when the silver concentration is low enough to prevent hoping of the olefin molecules from site-to-site in systems where fixed site carrier is the only facilitated transport mechanism. In composite membranes, the presence of the ionic liquid ensures transport facilitation *via* mobile carrier even at low silver concentrations.

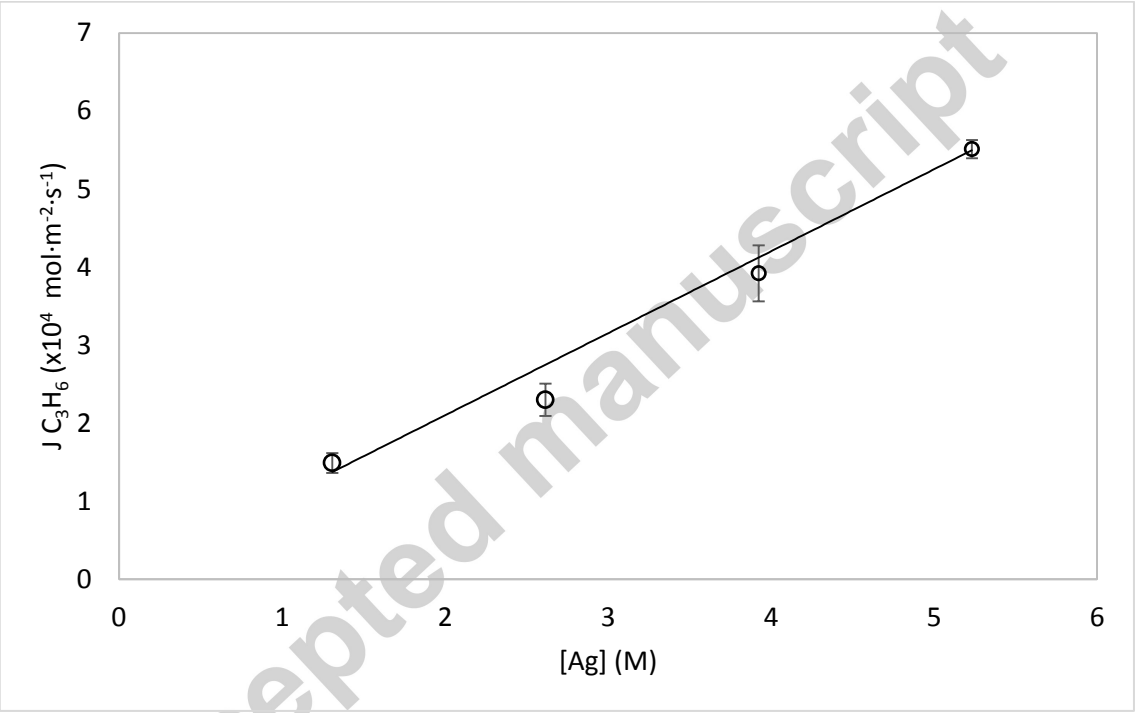

Figure 6. Experimental and predicted propylene flux in the PVDF-HFP/BMImBF$_4$/AgBF$_4$ membrane at 293K and a propylene feed partial pressure of 0.5 bar with increasing silver loading.

Figure 7 depicts the comparison between propylene and propane fluxes in a logarithmic scale. The noticeable difference between the flux values is due to two simultaneous phenomena, that is: in addition to the facilitated transport of propylene, the PVDF-HFP crystallinity reduces the paraffin physical solubility, yielding very low

flux via conventional solution-diffusion [45]. As a result, permeability selectivities higher than 150 are achieved, which satisfy the requirements for most of the industrial applications.

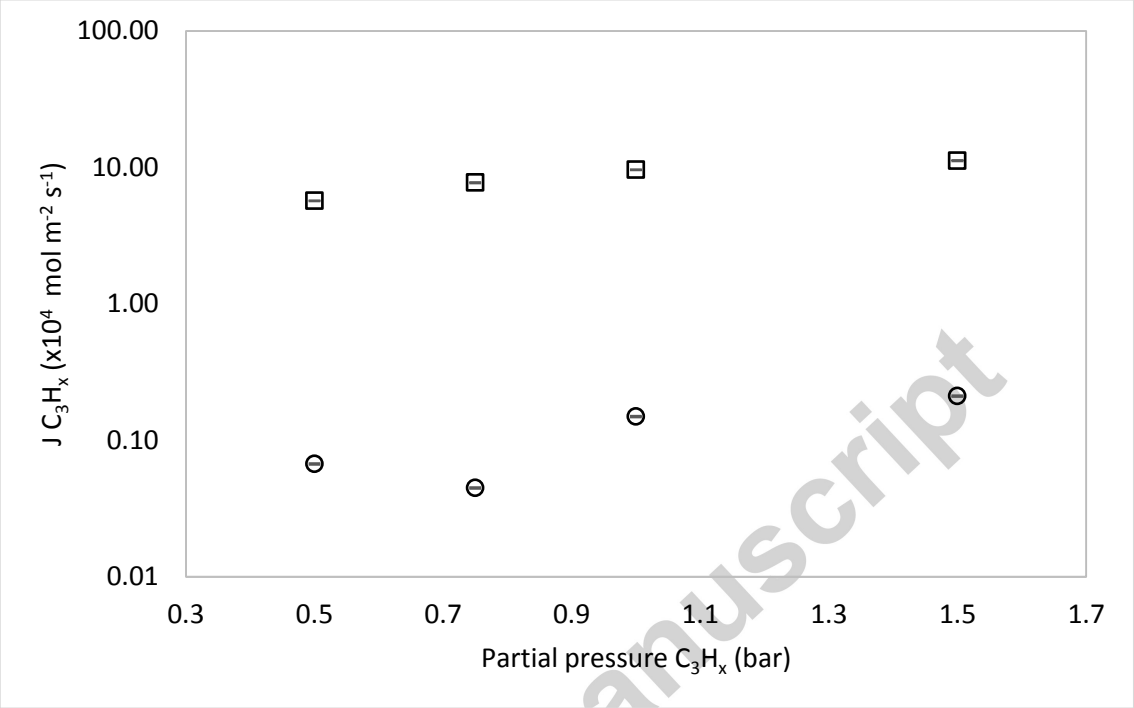

Figure 7. Propylene (□) and propane (○) experimental flux at 303 K in the PVDF-HFP/BMImBF$_4$/AgBF$_4$ 5.2 mol/L membrane with increasing feed partial pressure.

4.3 Model results

The model parameters taken from previous experimental studies are shown in Table 3. The proposed model has two estimated parameters: the fitting parameter α, and the fixed site carrier activation energy Ea_{FC}. Model regression to experimental data for each specific case study is needed in order to determine the values of these parameters. Aspen Custom Modeler software was employed in this work for estimation tasks. The resulting values of the fitting parameters for this particular case study are displayed in Table 4.

Table 3. Values of model parameters from previous works.

Parameter	Value	Reference
$D_{comp,ref}$ ($x10^{11}$ m^2 s^{-1})	3.22[a]	[22]
Ea_D (kJ mol^{-1})	7.13	[22]
k_p (bar^{-1})	0.12	[51]
$H_{C_3H_6,0}$ ($x10^3$mol bar^{-1} m^{-3})	4.28	[27]
ΔH_{sol} (kJ mol^{-1})	-24.1	[27]
$k_{eq,ref}$ (m^3 mol)	0.337[b]	[27]
ΔH_r (kJ mol^{-1})	-11.0	[27]

[a] The reference temperature is 293 K.

[b] The reference temperature is 278 K.

Table 4. Estimated model parameters.

Parameter	Value
Fixed-site carrier activation energy, Ea (kJ mol^{-1})	14.8
Fitting parameter, α ($x10^{11}$ m^2 bar^{-1} s^{-1})	1.35

Once the fitting parameters are obtained, the model is able to describe the system performance providing that the input data are within the studied range. Figures 4 and 6 compare the model predicted values to experimental data and prove the model accuracy to simulate the transmembrane flux for changing temperature, feed pressure and silver loading. The model values have been plotted against the experimental data to build the model parity graph, displaying a 10% error range, Figure 8. Besides, this generalized model is also capable of simulating the performance of SILMs when the fixed-site carrier contribution is neglected; in order to confirm this possibility, the parity graph includes the experimental and model results of supported ionic liquid membranes (SILMs) reported in previous works [22]. It can be seen that the majority of the points

fall within the acceptable error interval, suggesting an accurate fitting between the experimentally obtained values and the model calculations.

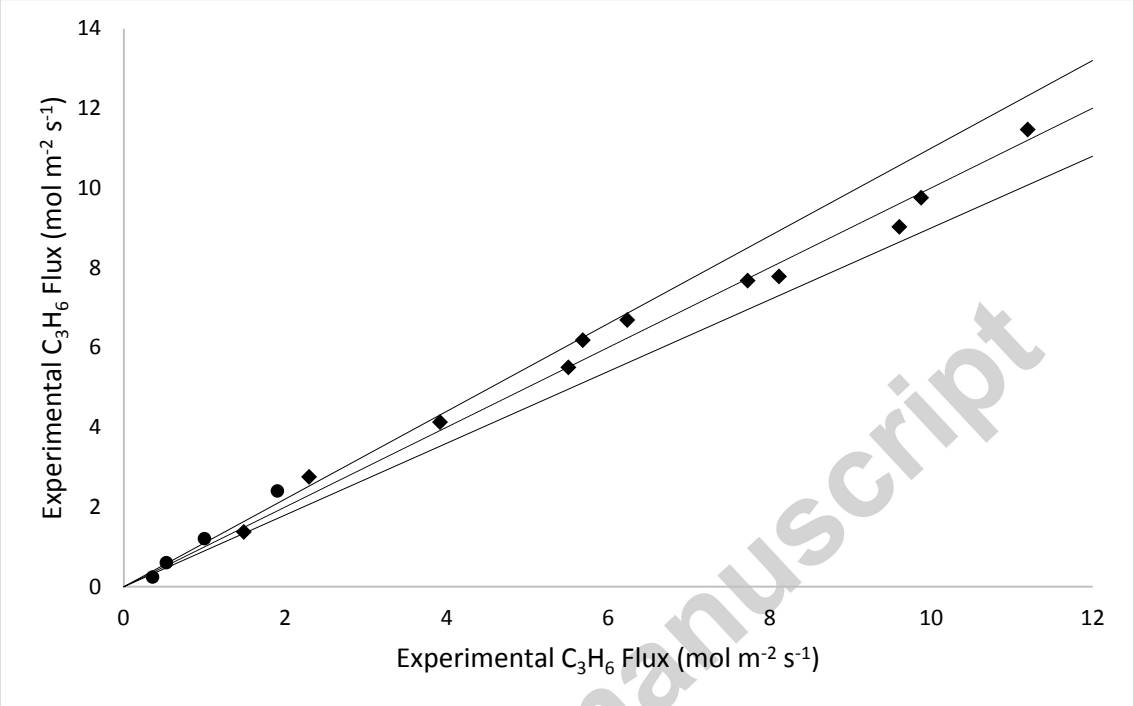

Figure 8. Model parity graph displaying a 10% error range: composite membranes (♦) SILMs (●).

With aim at the model application, it is also possible to extrapolate the model calculations out of the range of the studied variables, while taking into account the possible deviations associated with the extrapolation method. In this manner, the present model is a useful predictive tool to calculate the transmembrane flux in composite membranes performing a hybrid mobile/fixed carrier gas transport mechanisms. Figure 9 shows the predicted propylene flux in a wide range of propylene feed partial pressures and four temperatures for the highest silver loading assessed in this work. The values at pressures outside the 0.5-1.5 bar interval and at 283 and 313 K are model extrapolations. Process design and decision-making using composite membranes could

be improved implementing the proposed mathematical expressions to predict the material performance.

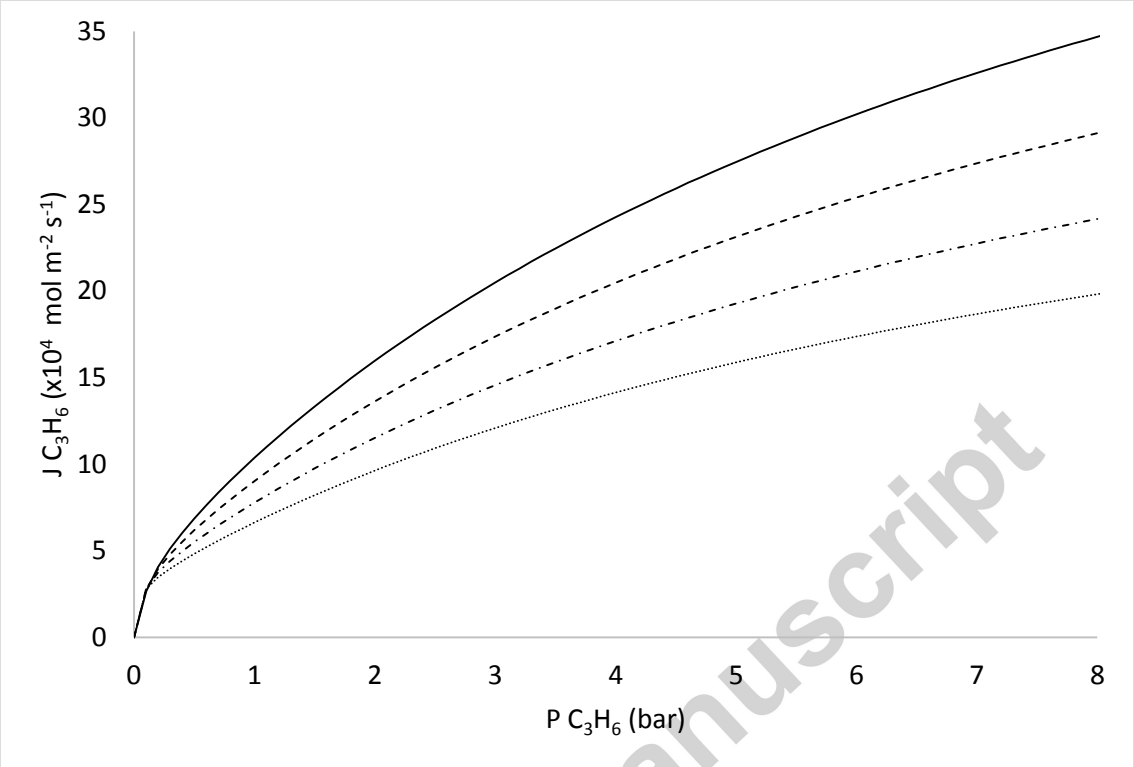

Figure 9. Propylene flux prediction in PVDF-HFP/BMImBF$_4$/AgBF$_4$ 5.23 M at 283 K (dot line); 293 K (dot-dash line); 303 K (dash line) and 313 K (solid line) over an extended propylene partial pressure range.

Finally, with the model, it is possible to calculate the contribution of the individual facilitated transport mechanisms to the total flux, as shown in Figure 10. The contribution of the solution-diffusion mechanism has been neglected because it represents less than 1% of the total flux in all cases. Note that the values at 283 K and 313 K have been extrapolated. The results show that, although the flux always shows an increasing trend with temperature, this variable has a greater effect on the fixed-site carrier mechanism compared to the mobile carrier. This behaviour is explained through the negative effect of temperature on the solubility term in the mobile carrier contribution.

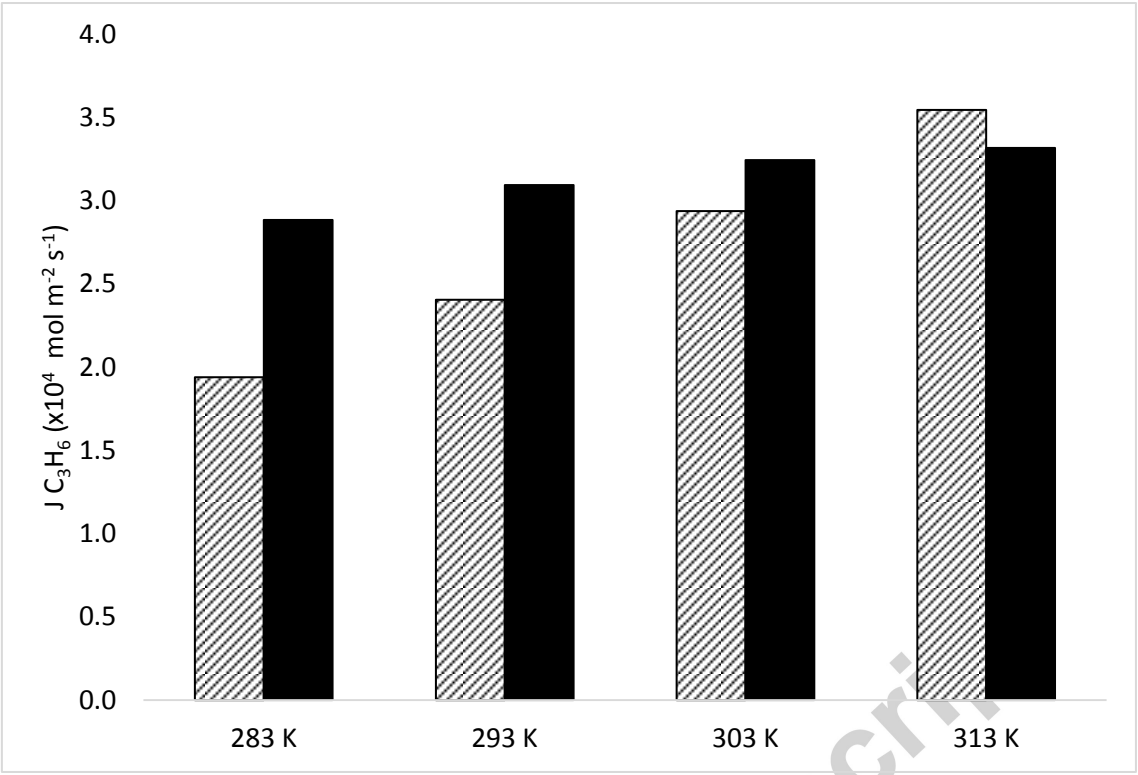

Figure 10. Predicted contribution of each facilitated transport mechanism to the total flux with increasing temperature at 0.5 bar propylene partial pressure in PVDF-HFP/BMImBF$_4$/AgBF$_4$ 5.23 M: fixed-site carrier (in stripes) and mobile carrier (in black).

5. Conclusions

A novel mathematical model able to describe the facilitated transport of propylene in composite membranes is reported. The model takes into account the different transport mechanisms featured in polymer/ionic-liquid/carrier systems, namely, solution-diffusion, fixed-site carrier and mobile carrier transport, describing the total gas flux as the sum of the contributions by each mechanism.

In order to check the suitability of the model simulated results where compared to experimental data obtained working with PVDF-HFP/$BMImBF_4$/$AgBF_4$ membranes in continuous-flow gas-mixture permeation tests, varying the temperature, silver loading and feed pressure. It has been checked that the addition of $BMImBF_4$ ionic liquid, which makes the membranes differ from solid state polymer electrolyte membranes, avoids the characteristic "percolation threshold" phenomena and allows transport facilitation even at low carrier concentration.

The model needs two fitting parameters $\alpha = 1.35 \times 10^{-11}$ m^2 bar^{-1} s^{-1} and Ea=14.8 kJ mol^{-1} that are case-sensitive depending on the chemical nature of the species (olefin, polymer, silver salt, ionic liquid) and their interactions. The reported model becomes a useful tool to predict the transmembrane flux via facilitated transport in those systems featuring fixed-site carrier and mobile carrier mechanisms simultaneously. In this regard, it will allow further design and optimization of more efficient membrane configurations.

Acknowledgement

Financial support from projects CTQ2015-66078-R and CTQ2016-75158-R (MINECO, Spain-FEDER 2014-2020) is gratefully acknowledged. Raúl Zarca also thanks the Universidad de Cantabria for a postgraduate fellowship.

5. Bibliography

[1] D.S. Sholl, R.P. Lively, Seven chemical separations to change the world, Nature. 532 (2016) 6–8.

[2] J.C. Charpentier, In the frame of globalization and sustainability, process intensification, a path to the future of chemical and process engineering (molecules into money), Chem. Eng. J. 134 (2007) 84–92.

[3] O.M. Ilinitch, G.L. Semin, M. V. Chertova, K.I. Zamaraev, Novel polymeric membranes for separation of hydrocarbons, J. Memb. Sci. 66 (1992) 1–8.

[4] K. Okamoto, A. Taguchi, J. Hao, K. Tanaka, H. Kita, Permeation and separation properties of polyimide membranes to olefins and paraffins, J. Memb. Sci. 121 (1996) 197–207.

[5] A. Ito, S.-T. Hwang, Permeation of propane and propylene thrugh cellulosic polymer membranes, J. Appl. Polym. Sci. 38 (1989) 483–490.

[6] R. Faiz, K. Li, Polymeric membranes for light olefin/paraffin separation, Desalination. 287 (2012) 82–97.

[7] R.J. Swaidan, X. Ma, E. Litwiller, I. Pinnau, Enhanced propylene/propane separation by thermal annealing of an intrinsically microporous hydroxyl-functionalized polyimide membrane, J. Memb. Sci. 495 (2015) 235–241.

[8] K.S. Liao, J.Y. Lai, T.S. Chung, Metal ion modified PIM-1 and its application for propylene/propane separation, J. Memb. Sci. 515 (2016) 36–44.

[9] V.F.D. Martins, A.M. Ribeiro, A. Ferreira, U.H. Lee, Y.K. Hwang, J.S. Chang, J.M. Loureiro, A.E. Rodrigues, Ethane/ethylene separation on a copper benzene-1,3,5-tricarboxylate MOF, Sep. Purif. Technol. 149 (2015) 445–456.

[10] M. Hartmann, U. Böhme, M. Hovestadt, C. Paula, Adsorptive Separation of Olefin/Paraffin Mixtures with ZIF-4, Langmuir. 31 (2015) 12382–12389.

[11] O. Salinas, X. Ma, Y. Wang, Y. Han, I. Pinnau, Carbon molecular sieve membrane from a microporous spirobisindane-based polyimide precursor with enhanced ethylene/ethane mixed-gas selectivity, RSC Adv. 7 (2017) 3265–3272.

[12] R.J. Swaidan, X. Ma, I. Pinnau, Spirobisindane-based polyimide as efficient precursor of thermally-rearranged and carbon molecular sieve membranes for enhanced propylene/propane separation, J. Memb. Sci. 520 (2016) 983–989.

[13] H.-X. Sun, B.-B. Yuan, P. Li, T. Wang, Y.-Y. Xu, Preparation of nanoporous graphene and the application of its nanocomposite membrane in propylene/propane separation, Funct. Mater. Lett. 8 (2015) 1550019.

[14] I. Pinnau, L.G. Toy, Solid polymer electrolyte composite membranes for olefin/paraffin separation, J. Memb. Sci. 184 (2001) 39–48.

[15] D.J. Safarik, R.B. Eldridge, Olefin/Paraffin Separations by Reactive Absorption: A Review, Ind. Eng. Chem. Res. 37 (1998) 2571–2581.

[16] A. Ortiz, L.M. Galán, D. Gorri, A.B. De Haan, I. Ortiz, Kinetics of reactive absorption of propylene in RTIL-Ag^+ media, Sep. Purif. Technol. 73 (2010) 106–113.

[17] M. Teramoto, H. Matsuyama, T. Yamashiro, Y. Katayama, Separation of Ethylene From Ethane By Supported Liquid Membranes Containing Silver-Nitrate As a Carrier, J. Chem. Eng. Japan. 19 (1986) 419–424.

[18] S. Duan, A. Ito, A. Ohkawa, Separation of propylene/propane mixture by a supported liquid membrane containing triethylene glycol and a silver salt, J. Memb. Sci. 215 (2003) 53–60.

[19] G. Zarca, I. Ortiz, A. Urtiaga, Copper(I)-containing supported ionic liquid membranes for carbon monoxide/nitrogen separation, J. Memb. Sci. 438 (2013) 38–45.

[20] M.T. Ravanchi, T. Kaghazchi, A. Kargari, Supported liquid membrane separation of propylene-propane mixtures using a metal ion carrier, Desalination. 250 (2010) 130–135.

[21] D. Gorri, M. Fallanza, A. Ortiz, I. Ortiz, Supported Liquid Membranes for Pervaporation Processes, in: Ref. Modul. Chem. Mol. Sci. Chem. Eng., 2017.

[22] M. Fallanza, A. Ortiz, D. Gorri, I. Ortiz, Experimental study of the separation of propane/propylene mixtures by supported ionic liquid membranes containing Ag^+–RTILs as carrier, Sep. Purif. Technol. 97 (2012) 83–89.

[23] T. Welton, Room-Temperature Ionic Liquids. Solvents for Synthesis and Catalysis, Chem. Rev. 99 (1999) 2071–2083.

[24] J.P. Hallett, T. Welton, Room-temperature ionic liquids: Solvents for synthesis and catalysis. 2, Chem. Rev. 111 (2011) 3508–3576.

[25] R. Faiz, K. Li, Olefin/paraffin separation using membrane based facilitated transport/chemical absorption techniques, Chem. Eng. Sci. 73 (2012) 261–284.

[26] J.H. Kim, S.W. Kang, Y.S. Kang, Threshold silver concentration for facilitated olefin transport in polymer/silver salt membranes, J. Polym. Res. 19 (2012).

[27] A. Ortiz, A. Ruiz, D. Gorri, I. Ortiz, Room temperature ionic liquid with silver salt as efficient reaction media for propylene/propane separation: Absorption equilibrium, Sep. Purif. Technol. 63 (2008) 311–318.

[28] A. Ortiz, L. Galán, D. Gorri, B. De Haan, I. Ortiz, Reactive Ionic Liquid Media for the Separation of Propylene / Propane Gaseous Mixtures, Ind. Eng. Chem. Res. 49 (2010) 7227–7233.

[29] M. Fallanza, A. Ortiz, D. Gorri, I. Ortiz, Polymer-ionic liquid composite membranes for propane/propylene separation by facilitated transport, J. Memb. Sci. 444 (2013) 164–172.

[30] L.C. Tomé, D. Mecerreyes, C.S.R. Freire, L.P.N. Rebelo, I.M. Marrucho, Polymeric ionic liquid membranes containing IL–Ag^+ for ethylene/ethane separation via olefin-facilitated transport, J. Mater. Chem. A. 2 (2014) 5631.

[31] R.D. Noble, Facilitated transport with fixed-site carrier membranes, J. Chem. Soc., Faraday Trans. 87 (1991) 2089–2092.

[32] R.D. Noble, Generalized microscopic mechanism of facilitated transport in fixed site carrier membranes, J. Memb. Sci. 75 (1992) 121–129.

[33] S. Najari, S.S. Hosseini, M. Omidkhah, N.R. Tan, Phenomenological modeling and analysis of gas transport in polyimide membranes for propylene/propane separation, RSC Adv. 5 (2015) 47199–47215.

[34] S. Sridhar, A.A. Khan, Simulation studies for the separation of propylene and propane by ethylcellulose membrane 1, 159 (1999) 209–219.

[35] M.T. Castoldi, Modeling of the Separation of Propene / Propane Mixtures by Permeation through Membranes in a Polymerization System, (2007) 1259–1269.

[36] M. Ohyanagi, H. Nishide, K. Suenaga, E. Tsuchida, Effect of Polymer Matrix and Metal Species on Facilitated Oxygen Transport in Metalloporphyrin (Oxygen Carrier) Fixed Membranes, Macromolecules. 21 (1988) 1590–1594.

[37] T. Suzuki, Y. Soejima, H. Nishide, E. Tsuchida, Effect of an oxygen-binding reaction at the cobalt porphyrin site fixed in a polymer membrane on facilitated oxygen transport, Bull. Chem. Soc. Jpn. 68 (1995) 1036–1041.

[38] D.R. Smith, J.A. Quinn, The facilitated transport of carbon monoxide through cuprous chloride solutions, AIChE J. 26 (1980) 112–120.

[39] R.D. Noble, Analysis of facilitated carrier membranes transport with fixed site, 50 (1990) 207–214.

[40] Y.S. Kang, J.M. Hong, J. Jang, U.Y. Kim, Analysis of facilitated transport in solid membranes with fixed site carriers: 1. Single RC circuit model, J. Memb. Sci. 109 (1996) 149–157.

[41] J.M. Hong, Y.S. Kang, J. Jang, U.Y. Kim, Analysis of facilitated transport in polymeric membrane with fixed site carrier: 2. Series RC circuit model, J. Memb. Sci. 109 (1996) 159–163.

[42] W.J. Ward, Analytical and experimental studies of facilitated transport, AIChE J. 16 (1970) 405–410.

[43] B.M. Johnson, R.W. Baker, S.L. Matson, K.L. Smith, I.C. Roman, M.E. Tuttle, H.K. Lonsdale, Liquid membranes for the production of oxygen-enriched air. II. Facilitated-transport membranes, J. Memb. Sci. 31 (1987) 31–67.

[44] M. Fallanza, M. González-Miquel, E. Ruiz, A. Ortiz, D. Gorri, J. Palomar, I. Ortiz, Screening of RTILs for propane/propylene separation using COSMO-RS methodology, Chem. Eng. J. 220 (2013) 284–293.

[45] S. Abbrent, J. Plestil, D. Hlavata, J. Lindgren, J. Tegenfeldt, Å. Wendsjö, Crystallinity and morphology of PVdF–HFP-based gel electrolytes, Polymer. 42 (2001) 1407–1416.

[46] H. Plenio, R. Diodone, Coordination Chemistry with CF Units as B Donors: Ag^{+} Complexes of Partially Fluorinated Crown Ethers with Direct Metal-Fluorine Interactions, Chem. Ber. 129 (1996) 1211–1217.

[47] P.K. Sazonov, L.K. Minacheva, A. V Churakov, V.S. Sergienko, G. a Artamkina, Y.F. Oprunenko, I.P. Beletskaya, Lariat ethers with fluoroaryl side-arms: a study of CFmetal cation interaction in the complexes of N-(o-fluoroaryl)azacrown ethers., Dalton Trans. (2009) 843–850.

[48] J. Chang, S.W. Kang, CO_2 separation through poly(vinylidene fluoride-co-hexafluoropropylene) membrane by selective ion channel formed by tetrafluoroboric acid, Chem. Eng. J. 306 (2016) 1189–1192.

[49] S. Sunderrajan, B.D. Freeman, C.K. Hall, I. Pinnau, Propane and propylene sorption in solid polymer electrolytes based on poly(ethylene oxide) and silver salts, J. Memb. Sci. 182 (2001) 1–12.

[50] R. Zarca, A. Ortiz, D. Gorri, I. Ortiz, Facilitated Transport of Propylene Through Composite Polymer-Ionic Liquid Membranes. Mass Transfer Analysis, Chem. Prod. Process Model. 11 (2016) 77–81.

[51] R. Zarca, A. Ortiz, D. Gorri, I. Ortiz, A practical approach to fixed-site-carrier facilitated transport modeling for the separation of propylene/propane mixtures through silver-containing polymeric membranes, Sep. Purif. Technol. 180 (2017) 82–89.

[52] J.H. Kim, B.R. Min, J. Won, Y.S. Kang, Complexation mechanism of olefin with silver ions dissolved in a polymer matrix and its effect on facilitated olefin transport, Chem. - A Eur. J. 8 (2002) 650–654.

[53] R. Surya Murali, K. Yamuna Rani, T. Sankarshana, A.F. Ismail, S. Sridhar, Separation of Binary Mixtures of Propylene and Propane by Facilitated Transport through Silver Incorporated Poly(Ether-Block-Amide) Membranes, Oil Gas Sci. Technol. – Rev. d'IFP Energies Nouv. 70 (2015) 381–390.

[54] Y. Yoon, J. Won, Y.S. Kang, Polymer electrolyte membranes containing silver ion for facilitated olefin transport, Macromolecules. 33 (2000) 3185–3186.

[55] A. Morisato, Z. He, I. Pinnau, T.C. Merkel, Transport properties of PA12-PTMO/$AgBF_4$ solid polymer electrolyte membranes for olefin/paraffin separation, Desalination. 145 (2002) 347–351.

Highlights:

Polymer/ionic liquid/silver salt membranes for olefin/paraffin gas separation.

Mathematical model to describe the olefin facilitated transport

Novel results of an experimental study at laboratory scale are reported.